Supporting Information

for

Two-stage electrolysis of H_2O and CO_2 to methanol: CO_2-to-methane reduction at the cathode and subsequent methane-to-methanol oxidation at the anode

Takashi Hibino *, Kazuyo Kobayashi, Masahiro Nagao, Zhou Dongwen, Chen Siyuan

Graduate School of Environmental Studies, Nagoya University, Nagoya 464-8601, Japan

Table of contents

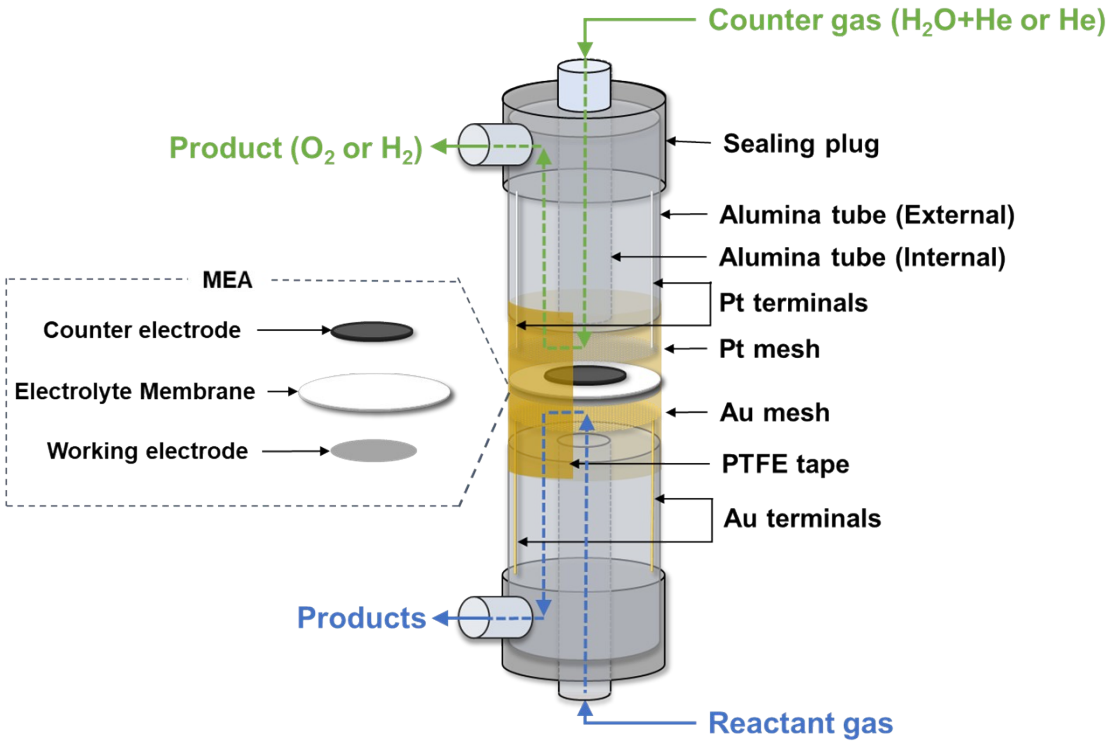

Figure S1. Schematic of the electrolysis cell used for the optimization of cathode and anode materials.

A mixture of CO_2 (20%) and He (80%) was fed into the cathode (working electrode), and a mixture of H_2O (6%) and He (94%) was fed into the anode for the synthesis of methane. A mixture of methane (20%), H_2O (6%), and He (balance) was fed into the anode (working electrode) and pure He was fed into the cathode for the synthesis of methanol. The flow rate of all the gases was maintained at 15 mL min^{-1}. In the membrane electrode assembly (MEA), the thickness of the electrolyte membrane and the area of the electrodes were 0.2 mm and 0.5 cm^2, respectively.

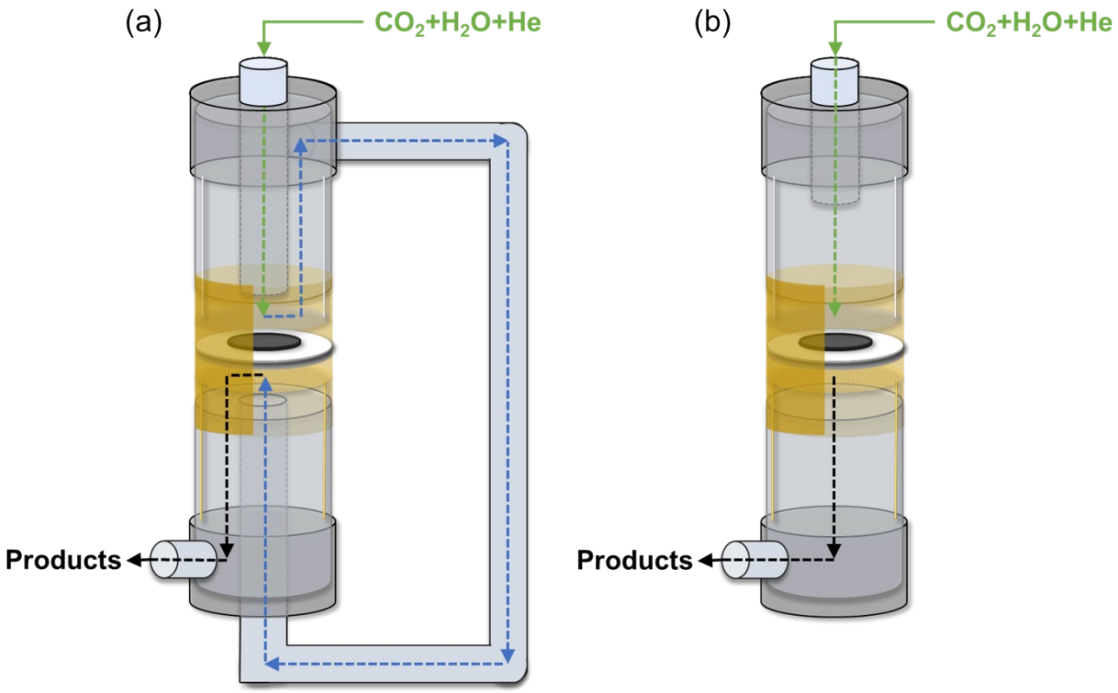

Figure S2. Schematics of the two-stage electrolysis cells used for the synthesis of methanol from H_2O and CO_2.

A mixture of CO_2 (20%), H_2O (6%), and He (balance) was fed from the cathode to the anode at a flow rate of 15 mL min^{-1}. Electrolyte membranes with thicknesses of 250 and 150 μm were used in Cells A and B, respectively. The gap between the 6-mm tube and the electrode was approximately 1 mm in Cell A.

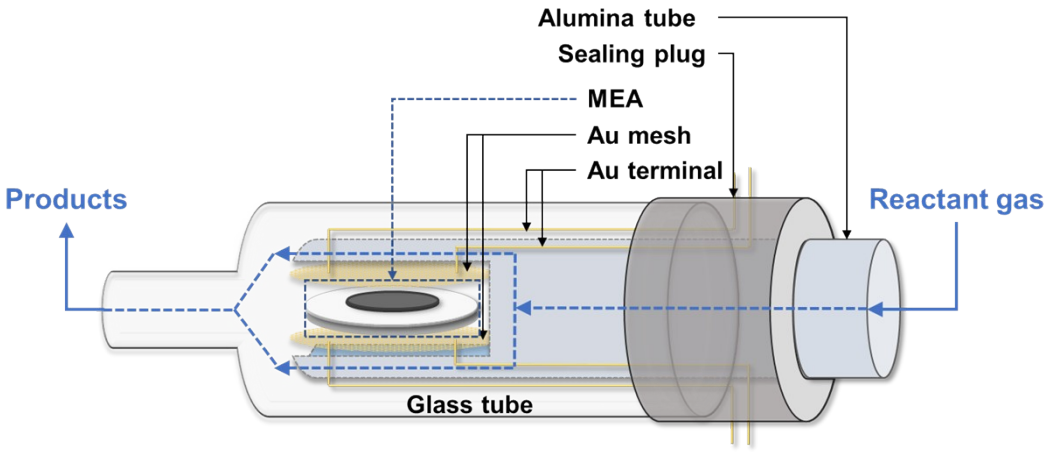

Figure S3. Schematic of the single-chamber electrolysis cell.

A mixture of methane (20%), H_2O (6%), and He (balance) was fed at a flow rate of 15 mL min^{-1} into both the anode and cathode of the cell placed horizontally in the single chamber, where one-half of the mixture was distributed to the anode and one-half to the cathode. A potential with an amplitude of +3 V and with various frequencies was applied to the electrochemical cell for the AC electrolysis.

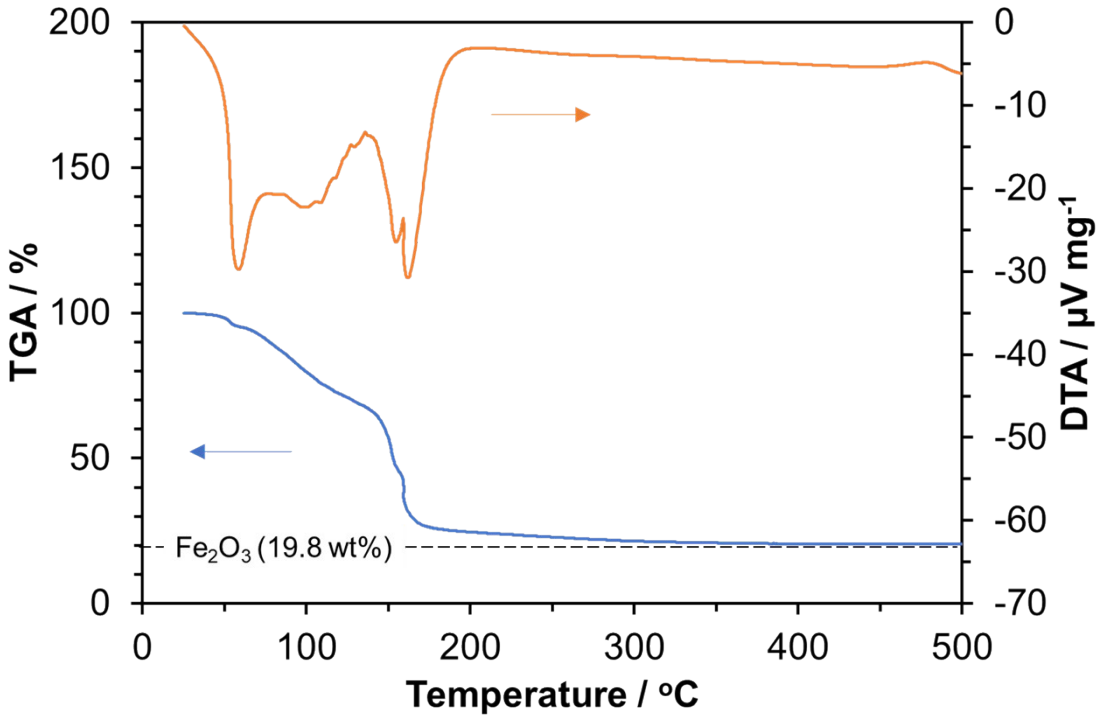

Figure S4. TG–DTA curves for iron(III) nitrate ($Fe(NO_3)_3 \cdot 9H_2O$).

The weight of iron(III) nitrate endothermically decreased to approximately 20 wt% until the temperature was 200 °C. When iron(III) nitrate decomposes to iron oxide, its weight becomes 19.8 wt% of the nitrate. Cerium(IV) nitrate, cobalt(II) nitrate, and indium(III) nitrate also decomposed to the corresponding metal oxides before the temperature reached 200 °C. These results are similar to those reported by Tagawa (Thermal decomposition of nitrates, Bulletin of the Institute of Environmental Science and Technology, Yokohama National University, 1987, 14, 41–57).

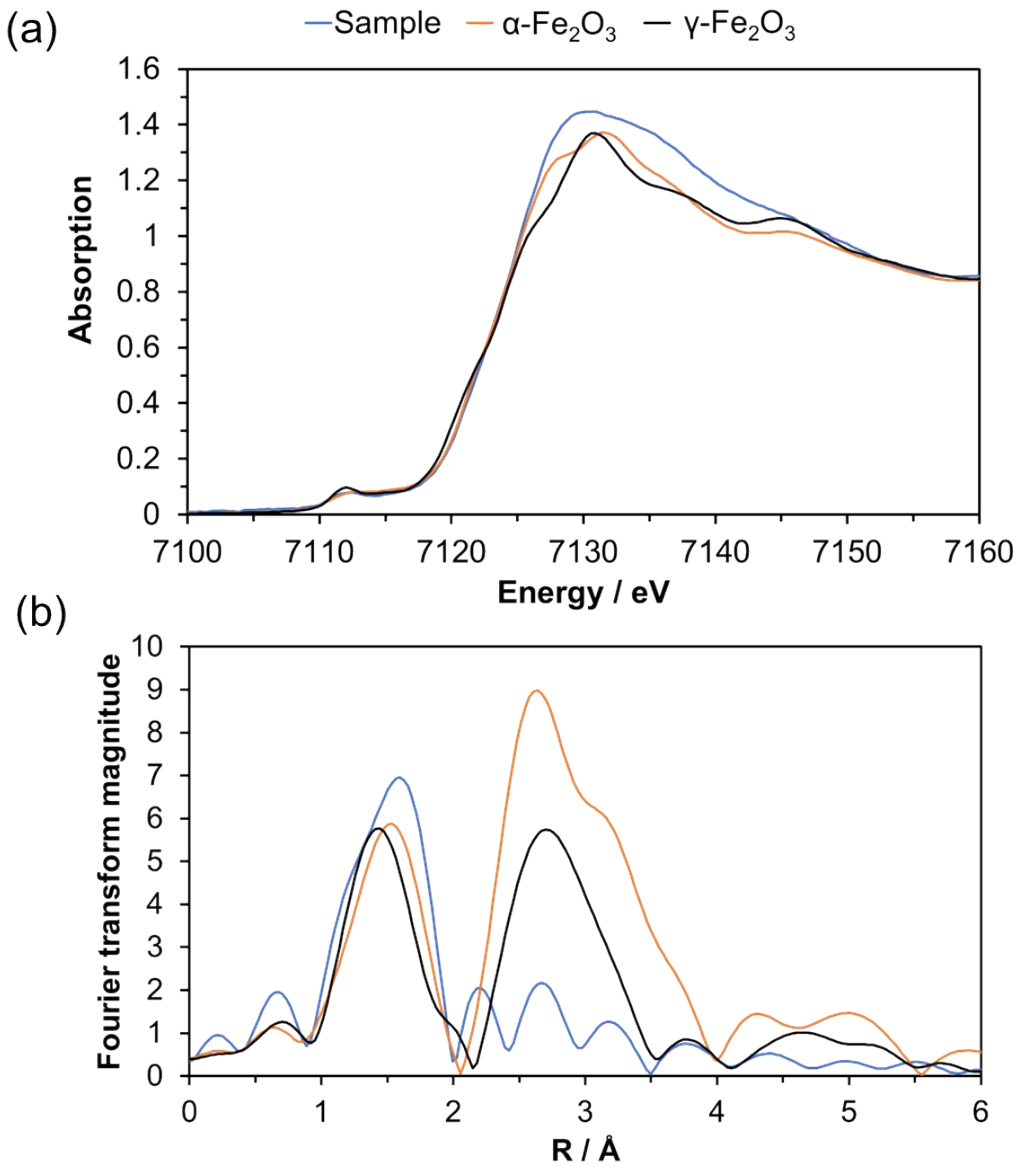

Figure S5. Fe-K-edge X-ray absorption fine structure spectra for the iron-impregnated Ru/C: (a) XANES and (b) Fourier transformed EXAFS.

The XANES and EXAFS spectra of the electrode sample indicated the presence of Fe(III), with a small pre-edge feature at 7112 eV, five first-shell oxygen neighbors, and an Fe–O distance of 1.98 Å. Therefore, the chemical state of iron in the cathode was consistent with that of iron in Fe_2O_3. However, the EXAFS spectra of the formed Fe_2O_3 showed a substantially weaker second neighbor peak than α- and γ-Fe_2O_3, which indicates that nanosized or amorphous Fe_2O_3 particles were deposited onto the carbon support.

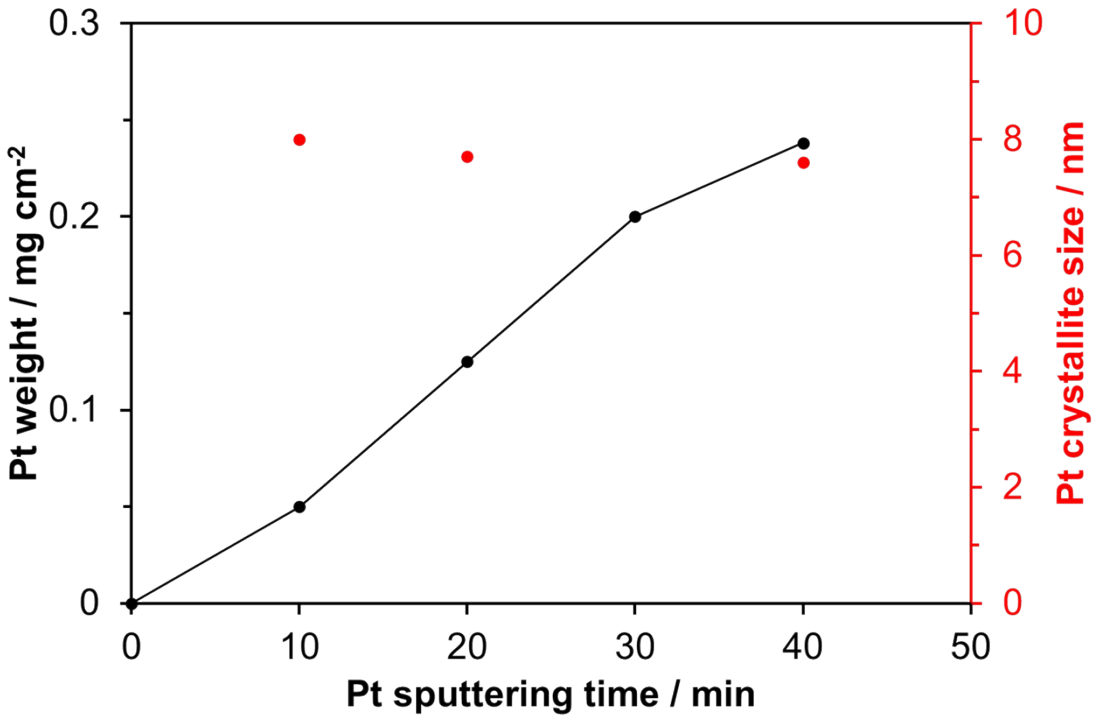

Figure S6. Changes in the Pt weight and crystallite size with sputtering time.

Although the weight of Pt increased linearly with increasing sputtering time, the average Pt crystallite size estimated from the XRD pattern was not strongly affected by the sputtering time. The Pt weight of the anode could therefore be adjusted using the sputtering time without altering the crystallite size. Notably, here, the sputtering rate (mg cm^{-2} min^{-1}) of metals, which corresponds to the slope of the linear relationship between the weight and time, is strongly dependent on the species of the metal targets.

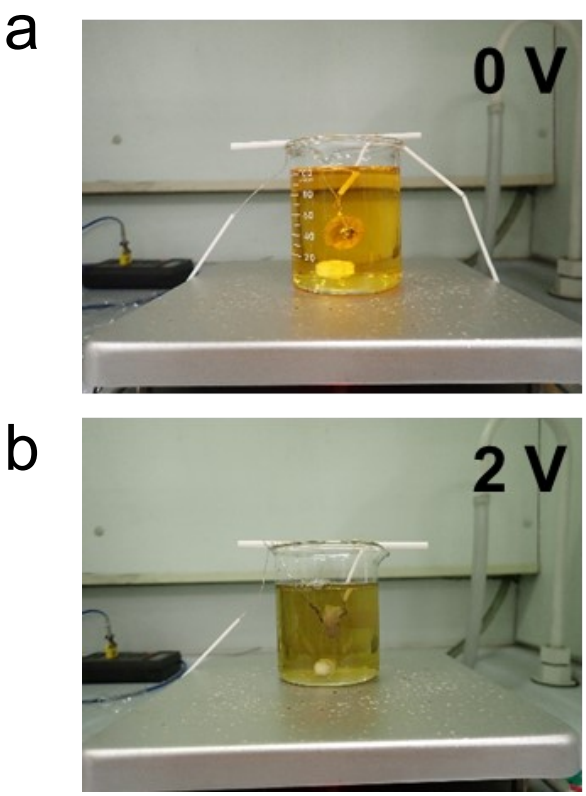

Figure S7. Change in the color of a phosphoric acid solution containing methyl violet as a result of the electrolysis of water. The electrochemical cell, Pt | $Sn_{0.9}In_{0.1}P_2O_7$ | Pt/C, was maintained for 3 h at (a) OCV or (b) +2 V.

Electrolysis of H_2O was conducted in a 100 mL phosphoric acid solution containing 30 μmol L^{-1} methyl violet without a supply of methane. The top of the beaker was sealed, and the bottom was heated at 200 °C. Most of the evaporated water condensed and returned to the beaker. The color of the solution became less intense when the cell was maintained +2 V than when it was maintained at OCV. Simultaneously, the UV absorbance of the solution was found to decrease as a result of the electrolysis (Figure 6(b)). These results indicate that •OH radicals were generated from water molecules during the electrolysis.

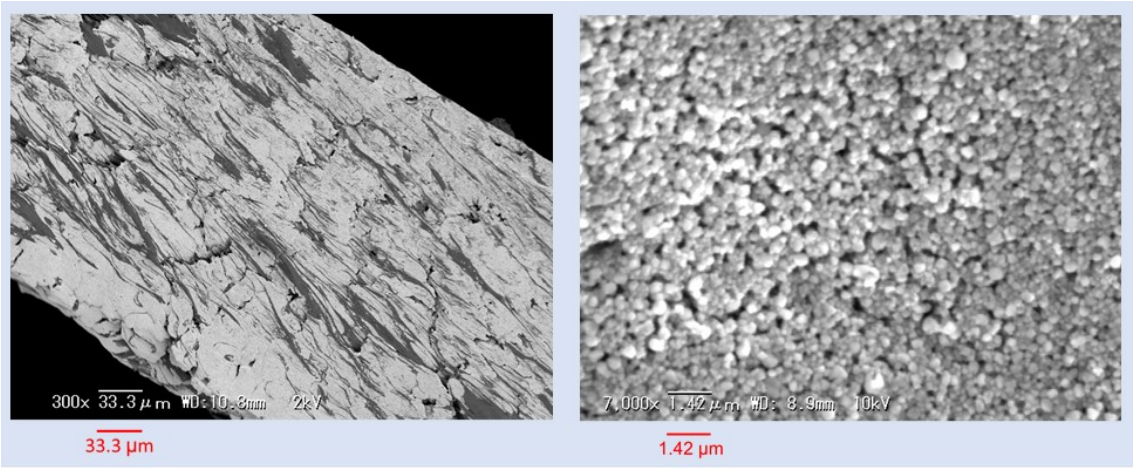

Figure S8. Cross-sectional SEM image (left) and top-view SEM image (right) of the electrolyte membrane.

The electrolyte membrane was mechanically supported on expanded PTFE (gray in the cross-sectional SEM image). The $Sn_{0.9}In_{0.1}P_2O_7$ particles were homogeneously and finely dispersed throughout the membrane, but not closely packed together (top-view SEM image). The formation of larger pores near the center than at the periphery might be due to the electron-beam irradiation of the specimens during the SEM observations.

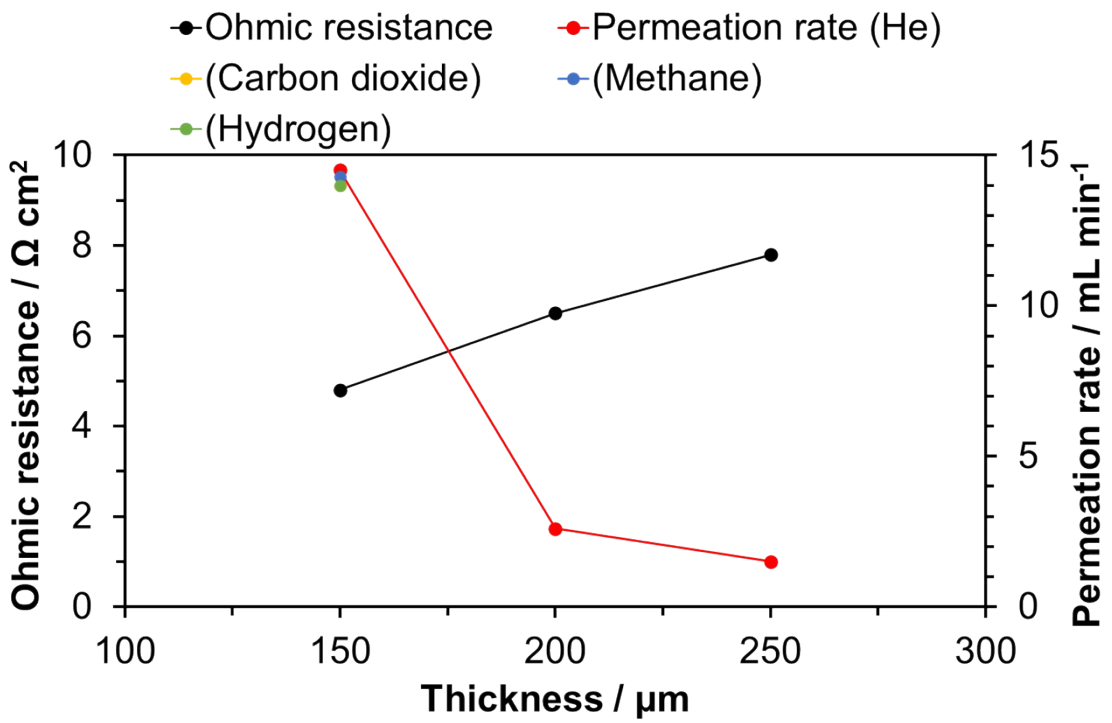

Figure S9. Ohmic resistance and He penetration rate as functions of the electrolyte membrane thickness. Data for CO_2, methane, and H_2 at a thickness of 150 μm are included for comparison.

As the thickness of the electrolyte membrane decreased, the ohmic resistance decreased and the He permeation rate increased. In particular, at a thickness of 150 μm, CO_2 (reactant gas), methane, and H_2 (cathode products), as well as He (carrier gas), permeated through the electrolyte membrane at sufficiently high rates. In addition, a roughly linear relationship was observed between each parameter and the membrane thickness. This observation is indirect evidence of the independent formation of three-dimensional networks of ionomers and pores in the membrane.

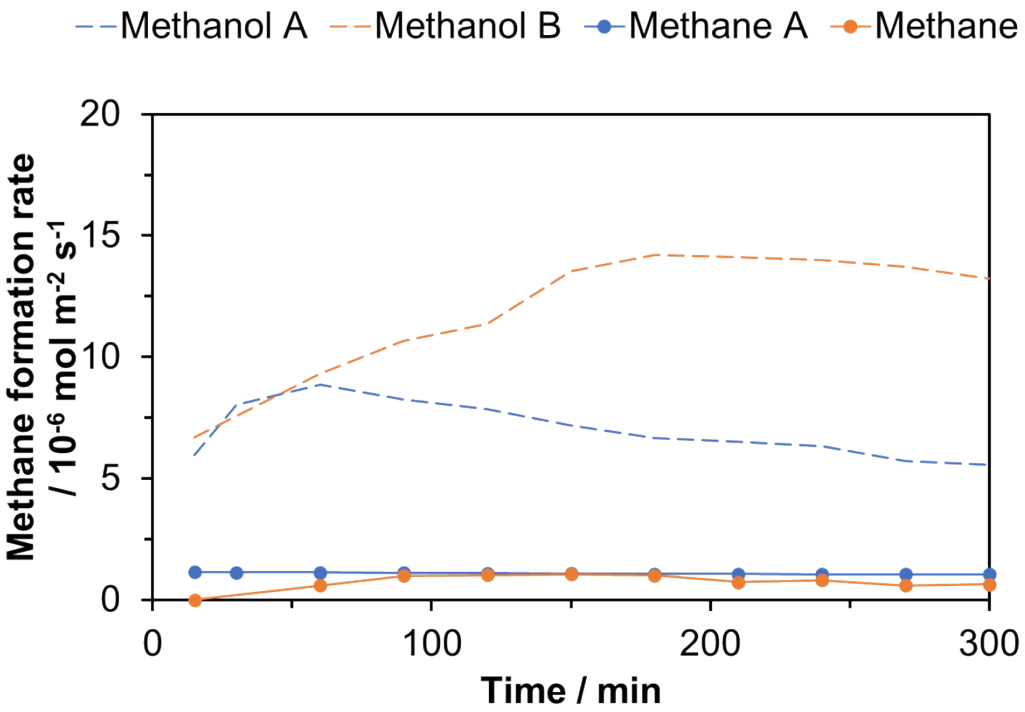

Figure S10. Changes in methane formation rate with time during electrolysis in Cells A and B at a cell voltage of 2.5 V. Data for the methanol formation rate are included for comparison.

The formation rates of methane for both the cells were much lower than those of methanol. We speculate that most of the methane formed at the cathode was oxidized to methanol at the anode.